

ORIGINAL  
RESEARCH

K.B. Walhovd  
A.M. Fjell  
J. Brewer  
L.K. McEvoy  
C. Fennema-Notestine  
D.J. Hagler, Jr  
R.G. Jennings  
D. Karow  
A.M. Dale,  
and the Alzheimer's  
Disease  
Neuroimaging  
Initiative



# Combining MR Imaging, Positron-Emission Tomography, and CSF Biomarkers in the Diagnosis and Prognosis of Alzheimer Disease

**BACKGROUND AND PURPOSE:** Different biomarkers for AD may potentially be complementary in diagnosis and prognosis of AD. Our aim was to combine MR imaging, FDG-PET, and CSF biomarkers in the diagnostic classification and 2-year prognosis of MCI and AD, by examining the following: 1) which measures are most sensitive to diagnostic status, 2) to what extent the methods provide unique information in diagnostic classification, and 3) which measures are most predictive of clinical decline.

**MATERIALS AND METHODS:** ADNI baseline MR imaging, FDG-PET, and CSF data from 42 controls, 73 patients with MCI, and 38 patients with AD; and 2-year clinical follow-up data for 36 controls, 51 patients with MCI, and 25 patients with AD were analyzed. The hippocampus and entorhinal, parahippocampal, retrosplenial, precuneus, inferior parietal, supramarginal, middle temporal, lateral, and medial orbitofrontal cortices were used as regions of interest. CSF variables included  $A\beta_{42}$ , t-tau, p-tau, and ratios of t-tau/ $A\beta_{42}$  and p-tau/ $A\beta_{42}$ . Regression analyses were performed to determine the sensitivity of measures to diagnostic status as well as 2-year change in CDR-SB, MMSE, and delayed logical memory in MCI.

**RESULTS:** Hippocampal volume, retrosplenial thickness, and t-tau/ $A\beta_{42}$  uniquely predicted diagnostic group. Change in CDR-SB was best predicted by retrosplenial thickness; MMSE, by retrosplenial metabolism and thickness; and delayed logical memory, by hippocampal volume.

**CONCLUSIONS:** All biomarkers were sensitive to the diagnostic group. Combining MR imaging morphometry and CSF biomarkers improved diagnostic classification (controls versus AD). MR imaging morphometry and PET were largely overlapping in value for discrimination. Baseline MR imaging and PET measures were more predictive of clinical change in MCI than were CSF measures.

**ABBREVIATIONS:**  $A\beta_{42}$  =  $\beta$  amyloid 1–42; AD = Alzheimer disease; ADNI = Alzheimer's Disease Neuroimaging Initiative; AUC = area under the curve; B = B coefficient for each predictor in the regression equation; CDR-SB = Clinical Dementia Rating sum of boxes; Corr. Class. = correlation classification; CSHC = Center for the Study of Human Cognition; FDA = US Food and Drug Administration; 18F-FDG = [ $^{18}$ F] fluorodeoxyglucose; FDG-PET = fluorodeoxyglucose-positron-emission tomography; inf. = inferior; lat. = lateral; LM-del = delayed Logical Memory from the *Wechsler Memory Scale Logical Memory II*; M = mean; MCI = mild cognitive impairment; med. orb. front. = medial orbital frontal; mid = middle; MMSE = Mini-Mental State Examination; MRI = MR imaging; NIH = National Institutes of Health; NC = healthy control; orb. front. = orbital frontal; p-tau = phosphorylated tau protein 181; parahippoc. = parahippocampus; PET = positron-emission tomography; t-tau = tau protein; ROC = receiver operating characteristics

Multiple biomarkers have proved sensitive to AD and MCI, a potential prodromal stage of AD. These include patterns of regional cerebral atrophy and hypometabolism detected by MR imaging and FDG-PET<sup>1</sup> and quantification of specific proteins in the CSF, including the tau protein and

$A\beta_{42}$ .<sup>2</sup> Tau is associated with axonal microtubules and is the main structural element of neurofibrils in AD. High CSF tau levels probably reflect axonal degeneration.<sup>3</sup>  $A\beta_{42}$  is derived from cleavage of amyloid precursor protein, and CSF  $A\beta_{42}$  levels are lowered early in AD, possibly due to sequestering of

Received May 20, 2009; accepted after revision July 1.

From Department of Psychology (K.B.W., A.M.F.), CSHC, University of Oslo, Oslo, Norway; Department of Neuropsychology (K.B.W., A.M.F.), Ullevål University Hospital, Oslo, Norway; Departments of Neuroscience (J.B., A.M.D.), Radiology (J.B., L.K.M., C.F.-N., D.J.H., R.G.J., D.K., A.M.D.), and Psychiatry (C.F.-N.), University of California, San Diego, La Jolla, California.


This work was supported by grants from the National Center for Research Resources (U24 RR021382-CFN, AMD, DJH) and the National Institute on Aging (R01AG22381-CFN, LKM, AMD; K01AG029218-LKM). The work of K.B. Walhovd and A.M. Fjell was supported by the Norwegian Research Council. Data collection and sharing for this project were funded by the ADNI (Principal Investigator, Michael Weiner; NIH grant U01 AG024904). The ADNI is funded by the National Institute on Aging, National Institute of Biomedical Imaging and Bioengineering, and through generous contributions from the following companies and organizations: Pfizer, Wyeth Research, Bristol-Myers Squibb, Eli Lilly and Company, GlaxoSmithKline, Merck & Co, AstraZeneca, Novartis Pharmaceuticals Corporation, the Alzheimer's Association, Eisai Global Clinical Development, Elan Corporation, Forest Laboratories, and the Institute for the Study of Aging with participation from the FDA. Industry partnerships are coordinated through the Foundation for the NIH. The grantee organization

is the Northern California Institute for Research and Education, and the study is coordinated by the Alzheimer's Disease Cooperative Study at the University of California, San Diego. ADNI data are disseminated by the Laboratory of Neuro Imaging at the University of California, Los Angeles.

Data used in the preparation of this article were obtained from the ADNI data base ([www.loni.ucla.edu/ADNI](http://www.loni.ucla.edu/ADNI)). As such, the investigators within the ADNI contributed to the design and implementation of ADNI and/or provided data but did not participate in the analysis or writing of this article. A complete listing of ADNI investigators is available at: [http://www.loni.ucla.edu/ADNI/Data/ADNI\\_Authorship\\_List.pdf](http://www.loni.ucla.edu/ADNI/Data/ADNI_Authorship_List.pdf).

Please address correspondence to Kristine B. Walhovd, MD, Department of Psychology, CSHC, University of Oslo, POB 1094 Blindern, 0317 Oslo, Norway; e-mail: [k.b.walhovd@psykologi.uio.no](mailto:k.b.walhovd@psykologi.uio.no)

 Indicates open access to non-subscribers at [www.ajnr.org](http://www.ajnr.org)

 Indicates article with supplemental on-line tables.

DOI 10.3174/ajnr.A1809

**Table 1: Demographic characteristics of the 3 subsamples<sup>a</sup>**

	NC (n = 42; 16F/26M)			MCI (n = 73, 25F/48M)			AD (n = 38, 16F/22M)		
	M	SD	Range	M	SD	Range	M	SD	Range
Age	75.5	(5.4)	62.2–84.7	74.5	(7.0)	55.5–88.9	76.2	(7.5)	58.8–88.1
Education	16.0	(3.2)	8–20	16.0	(2.9)	8–20	14.3	(3.6)	4–20
MMSE	29.1	(1.0)	26–30	27.0	(1.7)	24–30	23.8	(2.0)	20–26
MMSE_c	–0.2	(1.6)	–4–3	–1.3	(2.8)	–13–4	–5.2	(5.8)	–22–4
CDR	0.0	(0.0)	0–0	0.5	(0.0)	0.5–0.5	0.8	(0.3)	0.5–1.0
CDR_c	0.2	(0.7)	–0.5–3.5	1.2	(1.6)	–1.5–4.5	4.0	(3.1)	0–11
LM-del	12.0	(3.6)	6–22	4.1	(2.7)	0–8	1.1	(2.0)	0–8
LM-del_c	1.2	(4.1)	–10–8	0	(3.3)	–6–10	–0.7	(1.1)	–4–1

<sup>a</sup> The numbers refer to baseline data, with the exception of MMSE\_c, CDR\_c, and LM-del\_c, which refer to change across 2 years (baseline score subtracted from score at 2-year follow-up). MMSE and LM-del change scores were available for 36 NC, 51 MCI, and 25 AD subjects. CDR-SB change scores were available for 34 NC, 49 MCI, and 25 AD.

A $\beta$ 42 in neuritic plaques.<sup>4</sup> A full spectrum of imaging and CSF analysis methods is seldom used; thus, knowledge is limited on how they may best be combined. The ADNI, a large multisite study, was launched to enable analyses of combinations of different candidate biomarkers for AD.

Recent findings indicate that MR imaging can be used to quantify regional atrophy in MCI, distinguishing early and later preclinical stages of AD,<sup>5</sup> and such measures are predictive of clinical decline across 1 year.<sup>6–8</sup> A pattern of parieto-temporal metabolic reductions in MCI and AD and frontal metabolic reductions later in the disease has been established through the last decades of research<sup>1,9,10</sup> and has recently been confirmed in ADNI PET data.<sup>11</sup> The relative sensitivity of FDG-PET and MR imaging morphometry to AD-related changes is, however, not well established. It has been assumed that metabolic changes associated with neocortical dysfunction may be detectable by FDG-PET before atrophy appears. Consistent with this assumption, De Santi et al<sup>12</sup> reported that metabolism reductions exceeded volume losses in MCI, and Mosconi et al<sup>13</sup> found the same in presymptomatic early-onset familial AD. However, Jagust et al<sup>14</sup> found that cingulate hypometabolism was a significant risk factor in addition to MR imaging measures of hippocampal atrophy, but the latter was a more statistically robust risk factor in a group of cognitively impaired but not demented elderly.<sup>15</sup>

Different brain characteristics relevant for the understanding of MCI and AD may be captured by FDG-PET and MR imaging morphometry. For instance, a report based on ADNI data has indicated that FDG-PET and MR imaging measures may be complementary and differentially sensitive to memory in health and disease, with metabolism being the stronger predictor in healthy controls and morphometry most related to memory function in AD.<sup>16</sup> As for CSF–MR imaging relations, recent reports<sup>17–22</sup> indicate that cerebral anatomic differences are related to tau and A $\beta$ 42 and behavioral cognitive measures in AD and MCI. However, MR imaging and CSF biomarkers have not simultaneously been related and compared with information obtained by FDG-PET. It is important to test the specific sensitivity of all biomarkers simultaneously to be able to optimize the combination of measures in diagnosis and prognosis. We investigated the following: 1) which methods are the most sensitive to established AD-related pathology, 2) to what extent the methods provide unique-versus-overlapping information, and 3) which methods are the most predictive of clinical decline across 2 years.

## Materials and Methods

The raw data used in the preparation of this article were obtained from the ADNI data base ([www.loni.ucla.edu/ADNI](http://www.loni.ucla.edu/ADNI)). ADNI was launched in 2003 by the National Institute on Aging, the National Institute of Biomedical Imaging and Bioengineering, the FDA, private pharmaceutical companies, and nonprofit organizations. The primary goal of ADNI has been to test whether serial MR imaging, PET, other biologic markers, and clinical and neuropsychological assessment can be combined to measure the progression of MCI and early AD. The Principal Investigator of this initiative is Michael W. Weiner, of the Veterans Administration Medical Center and University of California-San Francisco. There are many coinvestigators, and subjects have been recruited from >50 sites across the United States and Canada. The ADNI has recruited 229 healthy elderly subjects, 398 patients with MCI, and 192 patients with AD to participate and be followed for 2–3 years. For up-to-date information, see [www.adni-info.org](http://www.adni-info.org).

## Sample

ADNI eligibility criteria are described at [http://www.adni-info.org/index.php?option=com\\_content&task=view&id=9&Itemid=43](http://www.adni-info.org/index.php?option=com_content&task=view&id=9&Itemid=43). Briefly, participants were 55–90 years of age, had an informant providing an independent evaluation of functioning, and spoke English or Spanish. Subjects were willing and able to undergo test procedures, including neuroimaging and longitudinal follow-up, and all gave informed consent. Specific psychoactive medications were excluded. General inclusion/exclusion criteria of the ADNI study are as follows: 1) healthy subjects: MMSE<sup>23</sup> scores between 24 and 30 inclusive (no person enrolled as an NC in the present sample had an MMSE score below 26); CDR of 0, nondepressed, non-MCI, and nondemented; 2) subjects with MCI: MMSE scores between 24 and 30 inclusive (exceptions made on a case-by-case basis, but no such exceptional cases were enrolled as patients with MCI in the present sample), a memory complaint, objective memory loss measured by *Wechsler Memory Scale Logical Memory II*,<sup>24</sup> CDR of 0.5, absence of significant levels of impairment in other cognitive domains, essentially preserved activities of daily living, and an absence of dementia; and 3) mild AD: MMSE scores between 20 and 26 inclusive (exceptions made on a case-by-case basis), CDR of 0.5 or 1.0, and met the National Institute of Neurological and Communicative Disorders and Stroke and the Alzheimer's Disease and Related Disorders Association criteria for probable AD.<sup>25</sup> Only ADNI subjects for whom adequate processed and quality checked MR imaging, FDG-PET, and CSF baseline data were available were included. This yielded a total of 153 participants. Demographics are shown in Table 1.

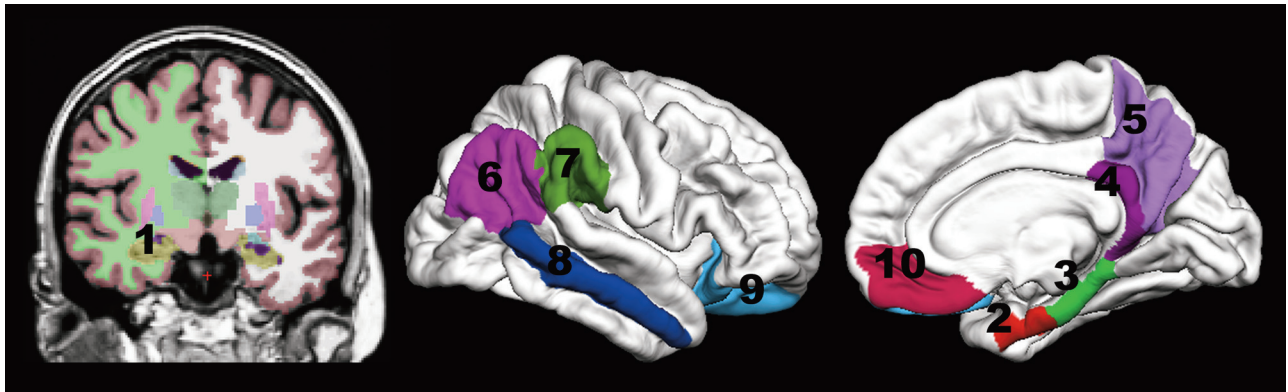


**Fig 1.** The regions of interest used are the following: 1) hippocampus and 2) entorhinal, 3) parahippocampal, 4) retrosplenial, 5) precuneus, 6) inferior parietal, 7) supramarginal, 8) middle temporal, 9) lateral orbitofrontal, and 10) medial orbitofrontal cortices.

### Standard Protocol Approvals, Registrations, and Patient Consents

The protocol was approved by the institutional review boards of participating sites. Written informed consent was obtained from all subjects or from guardians of patients.

### MR Imaging Acquisition and Analysis

All scans used here were from 1.5T scanners. Data were collected across a variety of scanners with protocols individualized for each scanner, as defined at <http://www.loni.ucla.edu/ADNI/Research/Cores/index.shtml>, and processed as described elsewhere.<sup>5,16</sup> Briefly, raw DICOM MR imaging scans (including 2 T1-weighted volumes per case) were downloaded from the ADNI site (<http://www.loni.ucla.edu/ADNI/Data/index.shtml>), reviewed for quality, automatically corrected for spatial distortion due to gradient nonlinearity<sup>26</sup> and B<sub>1</sub> field inhomogeneity,<sup>27</sup> registered, and averaged to improve signal intensity-to-noise ratios. Scans were segmented as described by Fischl et al,<sup>28</sup> yielding volumetric data for the hippocampal formation (consisting of the dentate gyrus, Cornu Ammonis fields, subiculum/parasubiculum, and the fimbria<sup>29</sup>).

The procedure<sup>28,30</sup> uses a probabilistic atlas and applies a Bayesian classification rule to assign a neuroanatomic label to each voxel. The cortical surface was reconstructed to measure thickness at each surface point by using a semiautomated approach described elsewhere.<sup>31-36</sup> Thickness measurements were obtained by reconstructing representations of the gray/white matter boundary<sup>31,32</sup> and the pial surface and then calculating the distance between those surfaces at each point across the cortical mantle. The measurement technique used here has been validated via histologic<sup>37</sup> and manual measurements.<sup>38</sup> The entire cortical surface was parcellated into numerous cortical areas.<sup>30,39</sup> To limit multiple comparisons, we selected candidate regions of interest on the basis of previous MR imaging and PET findings<sup>1,5,7,11,16,40-44</sup> indicating sensitivity to AD-related pathology: the hippocampi, and the entorhinal, parahippocampal, retrosplenial, precuneus, inferior parietal, supramarginal, middle temporal, and lateral and medial orbitofrontal gyri.

In the parcellation method used here,<sup>39</sup> the entire cingulate cortex was defined and divided into 4 separate regions, including the rostral and caudal anterior cingulate, the posterior cingulate, and the isthmus cingulate, the latter referred to here as the retrosplenial cortex for consistency with other published studies.<sup>5,16,40</sup> The retrosplenial region may also be referred to as the isthmus of the cingulate or caudal posterior cingulate area in other contexts. For a depiction of the exact regions of interest used, see Fig 1.

### FDG-PET Acquisition and Analysis

Subjects were scanned after a 4-hour fast (water only). Plasma glucose had to be  $\leq 180$  mg/dL for FDG to be injected. An intravenous catheter was placed in 1 arm for injection of 18F-FDG. Imaging began at 30 minutes postinjection, and the scan was acquired as six 5-minute frames. For each subject, FDG-PET frames were averaged and registered to the corresponding distortion-corrected and intensity-normalized MR imaging volume. PET activity for each subject was sampled onto their reconstructed cortical surface, averaged within each region of interest, and normalized to activity within the pons.<sup>45</sup>

### CSF Acquisition and Analysis

CSF samples obtained by lumbar puncture were examined for t-tau, p-tau, and A $\beta$ 42 by using an immunoassay method.<sup>46</sup> The measurements were performed by L. Shaw and J. Trojanowski of the ADNI Biomarker Core at the University of Pennsylvania School of Medicine. We analyzed the following CSF biomarkers for the present article: A $\beta$ 42 ( $202 \pm 56$ ,  $159 \pm 51$ ,  $136 \pm 39$  pg/mL for NC, MCI, and AD, respectively), t-tau ( $68 \pm 28$ ,  $100 \pm 65$ ,  $125 \pm 67$  pg/mL for NC, MCI, and AD, respectively), and p-tau ( $26 \pm 17$ ,  $36 \pm 19$ ,  $45 \pm 23$  for NC, MCI, and AD, respectively). The ratios of tau and A $\beta$ 42 (tau/A $\beta$ 42;  $0.37 \pm 0.21$ ,  $0.74 \pm 0.67$ ,  $0.98 \pm 0.56$  for NC, MCI, and AD, respectively) and the p-tau A $\beta$ 42 ratio (p-tau/A $\beta$ 42;  $0.16 \pm 0.16$ ,  $0.26 \pm 0.19$ ,  $0.36 \pm 0.22$  for NC, MCI, and AD, respectively) were also included. A 1-way analysis of variance on the residual CSF values after age and sex were regressed out showed significant ( $P < .001$ ) main effects of group on all variables. Post hoc tests controlling for multiple comparisons showed significant ( $P < .05$ ) differences between NC and MCI, NC and AD, and MCI and AD, with a few exceptions where trends ( $P < .10$ ) were observed (differences in t-tau between MCI and AD, p-tau between NC and MCI, and t-tau/A $\beta$ 42 between MCI and AD).

### Clinical and Cognitive Measures

Change scores were calculated by subtracting baseline scores from scores obtained at the 2-year follow-up. In addition to CDR-SB<sup>47</sup> and MMSE,<sup>23</sup> delayed recall on the *Wechsler Memory Scale-Revised*<sup>48</sup> was included. This test requires the subject to recall a story read by the examiner after a 30- to 40-minute delay and is sensitive to the episodic memory deficits in MCI.

### Statistics

A repeated-measures general linear model with the 10 regions of interest  $\times$  hemisphere (left, right)  $\times$  diagnostic group (NC, MCI, AD)

**Table 2: Results from logistic regression analyses for each method predicting NC versus AD**

Method	Step	Measure	B	P	Odds Ratio	% Corr. Class.	R <sup>2a</sup>	
MRI	1	Hippocampus	-2.306	.000	.100	NC:83.3 AD:81.6 All: 82.5	.601	
	2	Hippocampus	-2.291	.000	.101	NC:88.1	.665	
		Retrosplenial cortex	-1.202	.014	.301	AD:78.9 All: 83.8		
	3	Hippocampus	-1.581	.011	.206	NC:85.7	.714	
		Entorhinal cortex	-1.314	.026	.269	AD:84.2		
		Retrosplenial cortex	-1.230	.024	.292	All: 85.0		
	PET	1	Entorhinal cortex	-1.627	.000	.197	NC:85.7 AD:73.7 All: 80.0	.461
		2	Entorhinal cortex	-2.142	.000	.117	NC:81.0	.506
			Lateral orbitofrontal cortex	.675	.048	1.964	AD:76.3 All: 78.8	
3		Entorhinal cortex	-2.094	.000	.123	NC:88.1	.620	
		Retrosplenial cortex	-1.866	.003	.155	AD:76.3		
		Lateral orbitofrontal cortex	1.701	.002	5.481	All: 82.5		
CSF		1	t- $\tau$ :A $\beta$ 42	2.775	.000	16.036	NC:85.7 AD:76.3 All: 81.2	.523

<sup>a</sup> R<sup>2</sup> is Nagelkerke R<sup>2</sup>.

with age and sex as covariates showed no significant effect of hemisphere across regions of interest ( $F[1,148] = 1.530, P = .218$ ) and no interaction of hemisphere  $\times$  diagnostic group ( $F[2,148] = 0.847, P = .431$ ). Hence, values were averaged across hemispheres, effects of age and sex were regressed out, and the standardized residuals were used in the analyses. Correlation analyses with MR, FDG-PET, and CSF measures were run to assess their covariance. To select the measures yielding the most explained variance for each method, we entered the values in 3 separate logistic stepwise regressions by using MR, PET, and CSF measures respectively, predicting NC versus AD. The selected MR, PET, and CSF variables were then entered simultaneously in multimethod stepwise logistic regression analyses predicting NC versus AD and NC versus MCI. Next, the variables identified by the NC-versus-AD classification analysis were correlated with 2-year follow-up CDR-SB, MMSE, and delayed logical memory change scores in the MCI group and were entered as predictors in stepwise regression analyses with the respective behavioral change scores as the dependent variables.

## Results

Correlation analyses in the MCI group for morphometry and metabolism for the 10 regions of interest and the 5 CSF variables showed no significant ( $P < .05$ , corrected for 10 region-of-interest comparisons) correlations among CSF variables and morphometry or metabolism in any region of interest, whereas moderate correlations were found between morphometric and metabolic measures for the hippocampus and entorhinal, retrosplenial, and inferior parietal regions (on-line Table).

Table 2 shows the results of the separate logistic stepwise regressions predicting NC-versus-AD classification on the basis of MR imaging, FDG-PET, and CSF measures. Hippocampal volume and entorhinal and retrosplenial thickness, for MR imaging, were included in the final model, yielding an overall classification accuracy of 85.0%, and approximately 71% explained variance (Nagelkerke R<sup>2</sup>). Entorhinal, retrosplenial, and lateral orbitofrontal metabolism, for FDG-PET, were in-

cluded in the final model, yielding an overall classification accuracy of 82.5% and approximately 62% explained variance. For CSF, the ratio of t-tau/A $\beta$ 42 was the single unique predictor, yielding an overall classification accuracy of 81.2%, and approximately 52% explained variance. Thus, hippocampal volume; entorhinal and retrosplenial thickness; entorhinal, retrosplenial, and lateral orbitofrontal metabolism; and t-tau/A $\beta$ 42 ratio were entered in a logistic regression analysis to classify NC versus AD, and the results are shown in Table 3.

In the final model, hippocampal volume, retrosplenial thickness, and t-tau/A $\beta$ 42-ratio were included as predictors, yielding an overall classification accuracy of 88.8% and approximately 78% explained variance. Figure 2 depicts the ROC curves for these variables when using 1 (hippocampal volume) versus a combination of 2 (hippocampal volume and t-tau/A $\beta$ 42-ratio) and all 3 variables (hippocampal volume, t-tau/A $\beta$ 42-ratio, and retrosplenial thickness) shown to be unique predictors of NC-versus-AD classification. Predicted values from logistic regressions were used for calculation of the ROC curves. Statistical comparisons of the AUCs of these classifiers were performed by using the method of Hanley and McNeil.<sup>49</sup> This approach yielded a significant difference ( $P < .05$ ) between the AUCs using hippocampal volume alone versus using hippocampal volume and t-tau/A $\beta$ 42 ratio in combination and hippocampal volume, t-tau/A $\beta$ 42 ratio, and retrosplenial thickness in combination. The difference of the AUCs using hippocampal volume and t-tau/A $\beta$ 42 ratio versus hippocampal volume, t-tau/A $\beta$ 42 ratio, and retrosplenial thickness in combination was clearly smaller and not significant ( $P > .05$ ). Note however, that all meaningful differences in AUCs (eg, in terms of sensitivity versus specificity causing the curves to cross) may not necessarily be captured as statistically significant. The same set of predictor variables was entered in an analysis to predict diagnostic classification for NC and MCI, which revealed that hippocampal volume and t-tau/A $\beta$ 42 ratio were unique predictors, yielding an overall classi-

**Table 3: Results from the multimodal logistic regression analyses predicting NC versus AD<sup>a</sup>**

Step	Measure	B	P	Odds Ratio	% Corr. Class	R <sup>2</sup>
1	MRI hippocampus	-2.306	.000	.100	NC: 83.3 AD: 81.6 All: 82.5	.601
2	MRI hippocampus t- $\tau$ :A $\beta$ 42	-2.029 2.141	.000 .001	.132 8.509	NC: 88.1 AD: 81.6 All: 85.0	.733
3	MRI hippocampus MRI retrosplenial t- $\tau$ :A $\beta$ 42	-1.861 -1.239 2.411	.002 .028 .002	.155 .290 11.140	NC: 90.5 AD: 86.8 All: 88.8	.778
NC vs MCI						
1	MR hippocampus	-1.360	.000	.257	NC: 54.8 MCI:80.8 All: 71.3	.312
2	MR hippocampus t- $\tau$ :A $\beta$ 42	-1.124 1.422	.000 .006	.325 4.146	NC: 64.3 MCI:87.7 All: 79.1	.399

<sup>a</sup> The variables explaining unique variance within each method, as listed in Table 2, were included in the set of predictor variables, i.e. for MR: hippocampal volume, retrosplenial, and entorhinal thickness; for PET: entorhinal, retrosplenial, and lateral orbitofrontal metabolism; and for CSF: the ratio of T-tau to Abeta 42. R<sup>2</sup> is Nagelkerke R<sup>2</sup>.

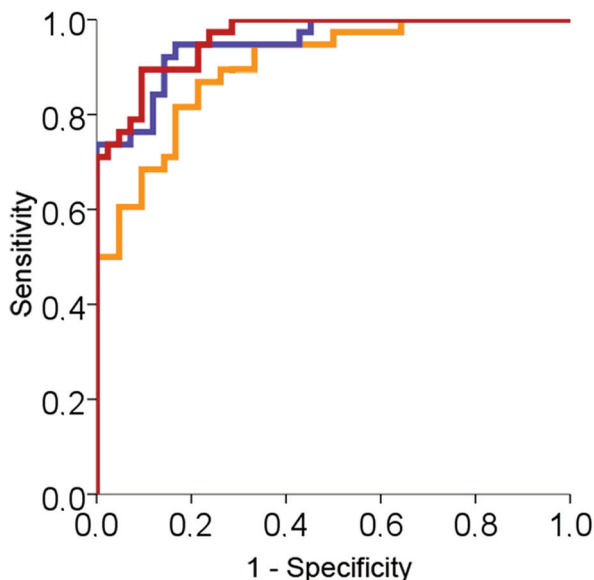


**Fig 2.** Comparison of ROC curves for using 1 versus a combination of 2 and all 3 variables shown to be unique predictors of NC-versus-AD classification. Yellow is the predicted probability based on hippocampal volume alone (AUC = 0.900, SE = 0.033). Blue is the predicted probability based on hippocampal volume and t-tau/A $\beta$ 42 ratio (AUC = 0.950, SE = 0.022). Red is the predicted probability based on hippocampal volume, t-tau/A $\beta$ 42 ratio, and retrosplenial cortical thickness (AUC = 0.961, SE = 0.018).

classification accuracy of 79.1% and approximately 40% explained variance.

Table 4 shows correlations for each variable included in the regression models and the cognitive change scores (CDR-SB, MMSE, delayed logical memory). In MCI, baseline retrosplenial thickness correlated with a 2-year change in CDR-SB and MMSE, where a thicker cortex was associated with less CDR-SB elevation and less MMSE reduction. Retrosplenial and entorhinal metabolism correlated negatively with MMSE change. Hippocampal volume correlated positively with delayed logical memory. There were no significant correlations with clinical change measures for t-tau/A $\beta$ 42 in MCI. *T* tests of the Fisher *z*-transformed correlation coefficients showed that the t-tau/A $\beta$ 42 ratio correlated significantly lower ( $P < .05$ ) with CDR-SB and MMSE change than did retrosplenial

**Table 4: Correlations between the variables included in the regression models predicting NC/AD classification and the change in CDR-SB ( $n = 49$ ) and MMSE ( $n = 51$ ) scores across 2 years in the MCI group<sup>a</sup>**

	CDR-SB Change	MMSE Change	LM-Del Change
MRI hippocampus	-.29	.29	.41 <sup>b</sup>
MRI entorhinal	-.17	.23	.34
MRI retrosplenial	-.43 <sup>b</sup>	.42 <sup>b</sup>	.35
PET entorhinal	-.30	.38 <sup>b</sup>	.28
PET retrosplenial	-.22	.47 <sup>b</sup>	.11
PET lat. orbitofrontal	-.02	.27	-.05
T- $\tau$ :A $\beta$ 42	.02	.08	-.23

<sup>a</sup> The variables explaining the unique variance within each method, as listed in Table 2, were included in the set of predictor variables (ie, for MR imaging, hippocampal volume and retrosplenial and entorhinal thickness; for PET, entorhinal, retrosplenial, and lateral orbitofrontal metabolism; and for CSF, the ratio of t-tau/A $\beta$ 42).  
<sup>b</sup>  $P < .05$ , corrected for 7 comparisons.

thickness and it correlated significantly lower with MMSE change than did entorhinal and retrosplenial metabolism. Lateral orbitofrontal metabolism also correlated significantly lower with change in CDR-SB and delayed logical memory than did retrosplenial thickness and hippocampal volume.

In the stepwise regression analysis predicting CDR-SB change, only retrosplenial cortical thickness was included as a unique predictor ( $y = 1.231 - 0.731x$ ,  $P = .002$ ), explaining 18% of the variance. In predicting MMSE change, retrosplenial metabolism was included in the first step ( $y = -1.193 + 1.534 x_1$ ,  $P = .002$  for  $x_1$ ,  $R^2 = 0.22$ ), and retrosplenial thickness was added in the second ( $y = -1.197 + 1.177x_1 + 0.776 x_2$ ,  $P = .009$  for  $x_1$  and  $.042$  for  $x_2$ ,  $R^2 = 0.29$ ). Only hippocampal volume was included as a predictor of delayed logical memory change ( $y = 0.240 + 1.669 x_1$ ,  $P = .003$  for  $x_1$ ,  $R^2 = 0.17$ ). The regression plots for CDR-SB and MMSE change predicted from retrosplenial thickness and metabolism and delayed logical memory predicted from hippocampal volume are shown in Fig 3. There was 1 outlier for the MMSE change score, with a 13-point decline. Without this outlier, only retrosplenial metabolism was included in the model for predicting MMSE change ( $y = -1.023 + 1.091 x_1$ ,  $P = .004$  for  $x_1$ ,  $R^2 = 0.16$ ), but a trend was observed for retrosplenial thickness ( $P = .079$ ).

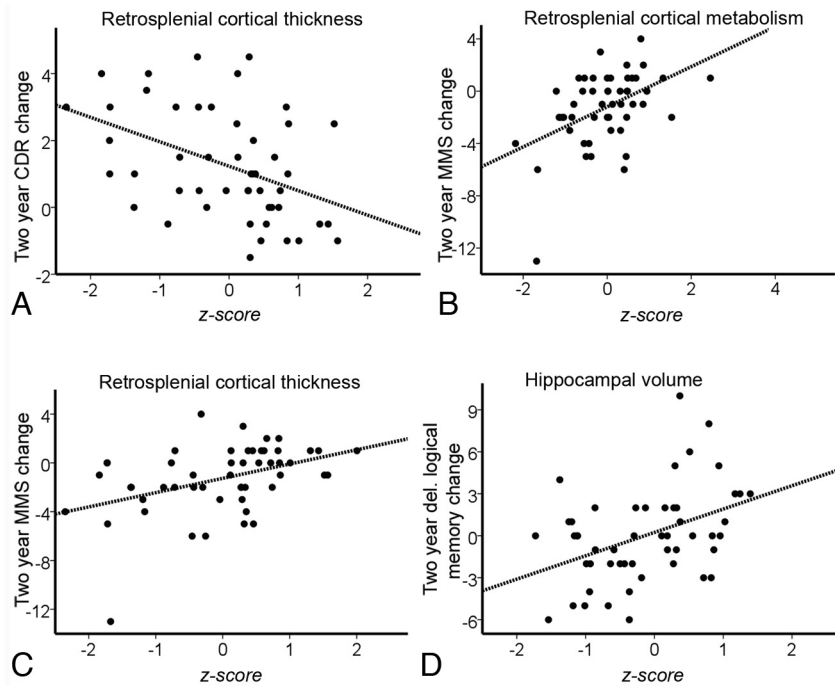


**Fig 3.** The regression plots for 2-year change in scores in the MCI group significantly ( $P < .05$ ) predicted from MR imaging morphometry and PET metabolism variables. *A*, CDR change predicted from retrosplenial cortical thickness. *B* and *C*, MMSE change predicted from retrosplenial cortical metabolism (*B*) and retrosplenial cortical thickness (*C*). *D*, Delayed logical memory change predicted from hippocampal volume.

## Discussion

Morphometry, metabolism, and CSF biomarkers were all sensitive to diagnostic status. The best classification accuracy of NC versus AD was obtained by MR imaging morphometry measures (hippocampal volume, entorhinal and retrosplenial cortical thickness). However, classification accuracies close to those obtained by MR imaging were also obtained by FDG-PET (entorhinal, retrosplenial, and lateral orbitofrontal metabolism) and CSF measures (t-tau/A $\beta$ 42-ratio). In the multimodal analysis, FDG-PET measures appeared to provide largely redundant information, whereas hippocampal volume, retrosplenial thickness, and the t-tau/A $\beta$ 42 ratio were unique predictors of diagnostic status. In particular, the inclusion of the CSF biomarker in addition to MR imaging hippocampal volume did result in a significant improvement in classification in terms of AUC. Thus, the combination of MR imaging morphometry and CSF biomarkers yielded the highest diagnostic classification accuracy. Contrary to this finding, in the prediction of clinical change during 2 years, FDG-PET and MR imaging morphometry were the best predictors. However, with the exception of retrosplenial metabolism and thickness in the prediction of change in MMSE scores, the 2 measures were largely redundant. Thus, it seems that the benefits of including both MR imaging morphometry and FDG-PET are modest in predicting clinical decline in MCI.

Whereas CSF biomarkers added to the diagnostic accuracy at baseline, they did not predict 2-year clinical decline in the current MCI group. This finding may be somewhat surprising because previous studies have found decreased CSF A $\beta$ 42 and/or tau or tau/A $\beta$ 42 levels to be predictive of future dementia in patients with MCI.<sup>2</sup> Several factors may have contributed to the discrepancies. First, the ongoing ADNI study may have a more heterogeneous MCI group than some of the

previously published CSF studies. As pointed out by Hansson et al,<sup>50</sup> participants included in CSF studies have generally been highly selected, for example, by inclusion of only patients with MCI who progress to AD. In ADNI, the ultimate end point is not known for many patients with MCI. Further, studies have often used dichotomized variables for CSF values and prognosis.<sup>50,51</sup> A stable/conversion dichotomization involves clinical judgment, which may vary from physician to physician and demands long follow-up intervals impractical for clinical trials. It may be advantageous to identify other preselection criteria, biomarkers, or clinical measures of decline than conversion. Therefore, it is important to relate the biomarkers to easily administered continuous behavioral measures. Most interesting, another study investigating continuous variables<sup>52</sup> did not find any association between MMSE change and change in CSF levels of either A $\beta$ 42, tau, or p-tau ( $r = 0.18, -.03, \text{ and } -.07$ , respectively). This does not mean that CSF measures are not related to clinical change. CSF tau/A $\beta$ 42 ratio did correlate in the expected negative direction with change in logical delayed memory in the present sample, but the effect size was too modest to reach significance. Select MR imaging morphometry and FDG-PET measures at baseline were significantly more sensitive to 2-year change in CDR-SB and MMSE than were CSF measures. Both cortical thickness and metabolism of parietal regions of interest served as unique predictors of clinical decline, indicating that even though FDG-PET did not contribute uniquely to diagnostic classification when MR imaging morphometric variance was accounted for, some additional prognostic information can be obtained by combining the 2 imaging modalities.

While the present findings show that the different biomarkers all were sensitive to diagnostic group, a question of great interest is whether the findings regarding specific measures

can be applied on an individual subject basis. McEvoy et al<sup>7</sup> recently reported that semiautomated individually specific quantitative MR imaging methods identical to those used here can be used to identify a pattern of atrophy in MCI that is predictive of conversion to AD after 1 year. Hence, in light of the present findings also indicating somewhat superior sensitivity of such MR imaging morphometry measures compared with other biomarkers, it does seem that these measures are prime candidates to be used on an individual basis (eg, to enrich clinical trials). However, as seen from Fig 3, while the MR imaging morphometry measures evaluated here do predict 2-year change in screening and memory parameters among patients with MCI, the regression plots also show considerable scatter. Hence, while these measures can yield individual prognostic information, this will be associated with considerable uncertainty, and at present, any such estimate must be made with great caution.

The present results are limited by a number of factors: Participants were selected on the basis of willingness and ability to undergo MR imaging and PET scanning and lumbar puncture and may thus not be fully comparable with other samples. However, imaging is an integral part of the ADNI protocol, so participants did enter with the intention of having brain scans performed, and approximately half of the ADNI participants have also agreed to have CSF samples drawn.<sup>53</sup> In terms of age, MMSE score, A $\beta$ 42, t-tau, p-tau, and ratios of t-tau/A $\beta$ 42 and p-tau/A $\beta$ 42, the subgroups studied in the present article do appear to be representative of the larger ADNI sample. The mean values for these indices in the present sample appear very similar to those reported by Shaw et al<sup>53</sup> for 410 participants with CSF measures, and all the present mean values for age, MMSE, and CSF measures for NC, MCI, and AD deviate less than one-fifth of the SDs from the means reported by Shaw et al for the larger groups. Still, the present sample may, of course, not be fully representative of the general population. Furthermore, the multisite design of the ADNI is likely to add some noise in data collection. Finally, the ADNI study is still ongoing, and the ultimate status of the current MCI group is unknown. That being said, the present study involving multiple sites and 2 years of follow-up likely represents a more realistic model for current clinical trial designs than longer interval single-site studies.

## Conclusions

Each of the biomarkers demonstrated potential to inform diagnosis and/or prognosis and enrich clinical trials. As a single classifier, MR imaging morphometry (hippocampal volume) was the most sensitive to diagnostic group, but the inclusion of CSF biomarkers (t-tau/A $\beta$ 42) did result in significant improvement of classification (NC/AD). Still, both quantitative MR imaging morphometry and regional metabolism as assessed by coregistered FDG-PET data provided better prediction of clinical decline than did CSF biomarkers. MR imaging morphometry showed somewhat superior diagnostic and prognostic sensitivity and is the least invasive, least expensive, and most widely available method. MR images are often routinely required as part of the diagnostic work-up, so a broader application of MR imaging morphometry may be feasible and useful.

## References

- Mosconi L, Brys M, Glodzik-Sobanska L, et al. Early detection of Alzheimer's disease using neuroimaging. *Exp Gerontol* 2007;42:129–38
- Craig-Schapiro R, Fagan AM, Holtzman DM. Biomarkers of Alzheimer's disease. *Neurobiol Dis* 2009;35:128–40. Epub 2008 Oct 28
- Blennow K, Wallin A, Agren H, et al. Tau protein in cerebrospinal fluid: a biochemical marker for axonal degeneration in Alzheimer disease? *Mol Chem Neuropathol* 1995;26:231–45
- Andreasen N, Blennow K. Beta-amyloid (A $\beta$ ) protein in cerebrospinal fluid as a biomarker for Alzheimer's disease. *Peptides* 2002;23:1205–14
- Fennema-Notestine C, Hagler DJ Jr, McEvoy LK, et al. Structural MRI biomarkers for preclinical and mild Alzheimer's disease. *Hum Brain Mapp* 2009;30:3238–53
- Leow AD, Yanovsky I, Parikshak N, et al. Alzheimer's disease neuroimaging initiative: a one-year follow up study using tensor-based morphometry correlating degenerative rates, biomarkers and cognition. *Neuroimage* 2009;45:645–55
- McEvoy LK, Fennema-Notestine C, Roddey JC, et al. Alzheimer disease: quantitative structural neuroimaging for detection and prediction of clinical and structural changes in mild cognitive impairment. *Radiology* 2009;251:195–205
- Misra C, Fan Y, Davatzikos C. Baseline and longitudinal patterns of brain atrophy in MCI patients, and their use in prediction of short-term conversion to AD: results from ADNI. *Neuroimage* 2009;44:1415–22
- Mosconi L, Tsui WH, Herholz K, et al. Multicenter standardized 18F-FDG PET diagnosis of mild cognitive impairment, Alzheimer's disease, and other dementias. *J Nucl Med* 2008;49:390–98
- de Leon MJ, Ferris SH, George AE, et al. Computed tomography and positron emission transaxial tomography evaluations of normal aging and Alzheimer's disease. *J Cereb Blood Flow Metab* 1983;3:391–94
- Langbaum JBS, Chen K, Lee W, et al. Categorical and correlational analyses of baseline fluorodeoxyglucose positron emission tomography images from the Alzheimer's Disease Neuroimaging Initiative. *Neuroimage* 2009;45:1107–16. Epub 2009 Jan 21
- De Santi S, de Leon MJ, Rusinek H, et al. Hippocampal formation glucose metabolism and volume losses in MCI and AD. *Neurobiol Aging* 2001;22:529–39
- Mosconi L, Sorbi S, de Leon MJ, et al. Hypometabolism exceeds atrophy in presymptomatic early-onset familial Alzheimer's disease. *J Nucl Med* 2006;47:1778–86
- Jagust WJ, Eberling JL, Wu CC, et al. Brain function and cognition in a community sample of elderly Latinos. *Neurology* 2002;59:378–83
- Wu CC, Mungas D, Petkov CI, et al. Brain structure and cognition in a community sample of elderly Latinos. *Neurology* 2002;59:383–91
- Walhovd KB, Fjell AM, Dale AM, et al. Multi-modal imaging predicts memory performance in normal aging and cognitive decline. *Neurobiol Aging* 2009. In press
- de Leon MJ, Mosconi L, Blennow K, et al. Imaging and CSF studies in the preclinical diagnosis of Alzheimer's disease. *Ann N Y Acad Sci* 2007;1097:114–45
- de Leon MJ, DeSanti S, Zinkowski R, et al. Longitudinal CSF and MRI biomarkers improve the diagnosis of mild cognitive impairment. *Neurobiol Aging* 2006;27:394–401
- Chou YY, Lepore N, Avedissian C, et al. Mapping correlations between ventricular expansion and CSF amyloid and tau biomarkers in 240 subjects with Alzheimer's disease, mild cognitive impairment, and elderly controls. *Neuroimage* 2009;46:394–410. Epub 2009 Feb 21
- Leow AD, Yanovsky I, Parikshak N, et al. Alzheimer's Disease Neuroimaging Initiative: a one-year follow up study using tensor-based morphometry correlating degenerative rates, biomarkers and cognition. *Neuroimage* 2009;45:645–55
- Schuff N, Woerner N, Boreta L, et al. MRI of hippocampal volume loss in early Alzheimer's disease in relation to ApoE genotype and biomarkers. *Brain* 2009;132(Pt 4):1067–77. Epub 2009 Feb 27
- Fjell AM, Walhovd KB, Amlien I, et al. Morphometric changes in the episodic memory network and tau pathologic features correlate with memory performance in patients with mild cognitive impairment. *AJNR Am J Neuroradiol* 2008;29:1183–89
- Folstein MF, Folstein SE, McHugh PR. "Mini-mental state": a practical method for grading the cognitive state of patients for the clinician. *J Psychiatr Res* 1975;12:189–98
- Wechsler, D. *Manual for the Wechsler Memory Scale-Revised*. The Psychological Corporation, San Antonio; 1987
- McKhann G, Drachman D, Folstein M, et al. Clinical diagnosis of Alzheimer's disease: report of the NINCDS-ADRDA Work Group under the auspices of Department of Health and Human Services Task Force on Alzheimer's Disease. *Neurology* 34:939–44
- Jovicich J, Czanner S, Greve D, et al. Reliability in multi-site structural MRI studies: effects of gradient non-linearity correction on phantom and human data. *Neuroimage* 2006;30:436–43
- Sled JG, Zijdenbos AP, Evans AC. A nonparametric method for automatic

- correction of intensity nonuniformity in MRI data. *IEEE Trans Med Imaging* 1998;17:87–97
28. Fischl B, Salat DH, Busa E, et al. **Whole brain segmentation: automated labeling of neuroanatomical structures in the human brain.** *Neuron* 2002;33:341–55
  29. Makris N, Meyer JW, Bates JF, et al. **MRI-based topographic parcellation of human cerebral white matter and nuclei. II. Rationale and applications with systematics of cerebral connectivity.** *Neuroimage* 1999;9:18–45
  30. Fischl B, van der Kouwe A, Destrieux C, et al. **Automatically parcellating the human cerebral cortex.** *Cereb Cortex* 2004;14:11–22
  31. Dale AM, Sereno MI. **Improved localization of cortical activity by combining EEG and MEG with MRI cortical surface reconstruction: a linear approach.** *J Cognitive Neurosci* 1993;5:162–76
  32. Dale AM, Fischl B, Sereno MI. **Cortical surface-based analysis. I. Segmentation and surface reconstruction.** *Neuroimage* 1999;9:179–94
  33. Fischl B, Dale AM. **Measuring the thickness of the human cerebral cortex from magnetic resonance images.** *Proc Natl Acad Sci U S A* 2000;97:11050–55
  34. Fischl B, Sereno MI, Dale AM. **Cortical surface-based analysis. II: Inflation, flattening, and a surface-based coordinate system.** *Neuroimage* 1999;9:195–207
  35. Fischl B, Sereno MI, Tootell RB, et al. **High-resolution intersubject averaging and a coordinate system for the cortical surface.** *Hum Brain Mapp* 1999;8:272–84
  36. Salat DH, Buckner RL, Snyder AZ, et al. **Thinning of the cerebral cortex in aging.** *Cereb Cortex* 2004;14:721–30
  37. Rosas HD, Liu AK, Hersch S, et al. **Regional and progressive thinning of the cortical ribbon in Huntington's disease.** *Neurology* 2002;58:695–701
  38. Kuperberg GR, Broome MR, McGuire PK, et al. **Regionally localized thinning of the cerebral cortex in schizophrenia.** *Arch Gen Psychiatry* 2003;60:878–88
  39. Desikan RS, Segonne F, Fischl B, et al. **An automated labeling system for subdividing the human cerebral cortex on MRI scans into gyral based regions of interest.** *Neuroimage* 2006;31:968–80
  40. Walhovd KB, Fjell AM, Amlien I, et al. **Multimodal imaging in mild cognitive impairment: metabolism, morphometry and diffusion of the temporal-parietal memory network.** *Neuroimage* 2009;45:215–23
  41. Edison P, Archer HA, Hinz R, et al. **Amyloid, hypometabolism, and cognition in Alzheimer disease: an [11C]PIB and [18F]FDG PET study.** *Neurology* 2007;68:501–08. Epub 2006 Oct 25
  42. Villain N, Desgranges B, Viader F, et al. **Relationships between hippocampal atrophy, white matter disruption, and gray matter hypometabolism in Alzheimer's disease.** *J Neurosci* 2008;28:6174–81
  43. Karas G, Sluimer J, Goekoop R, et al. **Amnesic mild cognitive impairment: structural MR imaging findings predictive of conversion to Alzheimer disease.** *AJNR Am J Neuroradiol* 2008;29:944–49
  44. Devanand DP, Habeck CG, Tabert MH, et al. **PET network abnormalities and cognitive decline in patients with mild cognitive impairment.** *Neuropsychopharmacology* 2006;31:1327–34
  45. Minoshima S, Frey KA, Foster NL, et al. **Preserved pontine glucose metabolism in Alzheimer disease: a reference region for functional brain image (PET) analysis.** *J Comput Assist Tomogr* 1995;19:541–47
  46. Shaw LM, Korecka M, Clark CM, et al. **Biomarkers of neurodegeneration for diagnosis and monitoring therapeutics.** *Nat Rev Drug Discov* 2007;6:295–303. Epub 2007 Mar 9
  47. Morris JC. **The Clinical Dementia Rating (CDR): current version and scoring rules.** *Neurology* 1993;43:2412–14
  48. Wechsler D. *Wechsler Memory Scale-Revised.* San Antonio: Psychological Corporation; 1987
  49. Hanley JA, McNeil BJ. **A method of comparing the areas under receiver operating characteristic curves derived from the same cases.** *Radiology* 1983;148:839–43
  50. Hansson O, Zetterberg H, Buchhave P, et al. **Association between CSF biomarkers and incipient Alzheimer's disease in patients with mild cognitive impairment: a follow-up study.** *Lancet Neurol* 2006;5:228–34
  51. Hansson O, Buchhave P, Zetterberg H, et al. **Combined rCBF and CSF biomarkers predict progression from mild cognitive impairment to Alzheimer's disease.** *Neurobiol Aging* 2009;30:165–73
  52. Sluimer JD, Bouwman FH, Vrenken H, et al. **Whole-brain atrophy rate and CSF biomarker levels in MCI and AD: a longitudinal study.** *Neurobiol Aging* 2008 Aug 7. [Epub ahead of print]
  53. Shaw LM, Vanderstichele H, Knapiak-Czajka M, et al. **Cerebrospinal fluid biomarker signature in Alzheimer's disease neuroimaging initiative subjects.** *Ann Neurol* 2009;65:403–13